DOI: 10.1002/cbic.200900251

Translational Diffusion and Interaction of a Photoreceptor and Its Cognate Transducer Observed in Giant Unilamellar Vesicles by Using Dual-Focus FCS

Jana Kriegsmann,[a] Ingo Gregor,[b] Iris von der Hocht,[c, e] Johann Klare,[d] Martin Engelhard,[d] Jörg Enderlein,[b] and Jörg Fitter*[a]

In order to monitor membrane–protein binding in lipid bilayers at physiological protein concentrations, we employed the recently developed dual-focus fluorescence correlation spectroscopy (2fFCS) technique. In a case study on a photoreceptor consisting of seven transmembrane helices and its cognate transducer (two transmembrane helices), the lateral diffusion for these integral membrane proteins was analyzed in giant unilamellar vesicles (GUVs). The two-dimensional diffusion coefficients of both separately diffusing proteins differ significantly, with $D = 2.2 \times 10^{-8}\,cm^2\,s^{-1}$ for the photoreceptor and with $D = 4.1 \times 10^{-8}\,cm^2\,s^{-1}$ for the transducer. In GUVs with both membrane proteins present together, we observed significantly smaller diffusion coefficients for labelled transducer molecules; this indicates the presence of larger diffusing units and therefore intermolecular protein binding. Based on the phenomenological dependence of diffusion coefficients on the molecule's cylindrical radius, we are able to estimate the degree of membrane protein binding on a quantitative level.

Introduction

Membrane proteins have to cope with various specific tasks in the cell. They ensure interaction and communication of the cell with its environment by forming channels or providing receptor molecules that transfer various kinds of information. In order to fulfil these requirements, larger oligomeric protein complexes often need to be formed in the cell membrane. A well studied example in this respect is given by a photoreceptor (NpSRII) and its cognate transducer (NpHtrII). Together they form a photo-signaling complex in *Natronomonas pharaonis*.[1,2] NpSRII consists of seven membrane-spanning α-helices, while NpHtrII is made up of two membrane-spanning helices and a cytoplasmic domain composed of a coiled-coiled four-helix bundle. EPR-spectroscopy and crystallographic studies on the Np(SRII–HtrII)-complex with a truncated version of the transducer ($NpHtrII_{157}$, which is missing the cytoplasmic domain) indicated that NpSRII and NpHtrII form a 2:2 complex with a twofold symmetry axis perpendicular to the lipid membrane surface. This complex formation is facilitated by the intermolecular binding of transmembrane transducer helices.[3,4] According to these results the 2:2 complex is assumed to be the functional unit and both Np(SRII–HtrII) and Np(HtrII–HtrII) binding are essential to form the complex. Recent Förster resonance energy transfer (FRET) measurements at protein concentrations (molar protein/lipid ratios: 1:200–8000) much lower than those used in electron paramagnetic resonance (EPR) and crystallographic studies (typical protein/lipid ratio: 1:50) revealed much stronger Np(SRII–HtrII) binding than Np(HtrII–HtrII) binding.[5] Most likely, the cytoplasmic transducer domain (missing in the above-mentioned studies) is essential to ensure a stronger Np(HtrII–HtrII) binding, which is required to obtain functional photosignalling complexes in the cell. However, in the cell the concentration of photoreceptors is even lower, with approximately 400 molecules per cell;[6] this corresponds to a molar protein lipid ratio on the order of 1:1 000 000. To achieve such low protein concentrations in a lipid bilayer system we incorporated the membrane proteins into giant unilamellar vesicles (GUV) for membrane–protein binding studies. GUVs, which have an average size (diameter ~10–40 μm) very similar to that of cells, have often been used as well-defined cell membrane models.[7,8] In contrast to supported lipid bilayers in which the bilayer may interact with the solid support, GUVs provide a free standing (top) bilayer.[9,10] This advantage is valuable for determining the precise lateral diffusion of integral membrane proteins and for analyzing membrane protein binding in an unperturbed environment. To measure how such protein complexes are formed in lipid bilayers at physiological protein concentrations is still an experimental challenge. Advanced spectroscopic techniques such as fluorescence correla-

[a] *Dr. J. Kriegsmann, Dr. J. Fitter*
Research Centre Jülich, ISB 2: Molecular Biophysics
52425 Jülich (Germany)
Fax: (+49) 2461-611448
E-mail: j.fitter@fz-juelich.de

[b] *Dr. I. Gregor, Prof. J. Enderlein*
Georg August University Göttingen, III. Institute of Physics
37077 Göttingen (Germany)

[c] *Dr. I. von der Hocht*
Research Centre Jülich, ISB 1: Cellular Biophysics
52425 Jülich (Germany)

[d] *Dr. J. Klare, Prof. M. Engelhard*
Max-Planck Institute of Molecular Physiology
44227 Dortmund (Germany)

[e] *Dr. I. von der Hocht*
Present address: Max-Planck Institute of Biophysics
60438 Frankfurt (Germany)

tion spectroscopy (FCS), single particle tracking, as well as other kinds of single molecule techniques have been successfully applied to investigate proteins in artificial lipid bilayer systems or in cell membranes.[11–16] Here we applied the recently developed dual-focus FCS (2fFCS) technique[17] to measure the lateral diffusion of integral membrane proteins in GUVs. The measurement of changes in the diffusion coefficients between samples of labelled transducer molecules in the absence or presence of nonlabelled receptor molecules allowed the detection of intermolecular protein binding.

Results and Discussion

GUVs and membrane protein incorporation

For the incorporation of functional membrane proteins into GUVs, we fused proteoliposomes with fluorescently labelled membrane proteins onto surface-tethered GUVs (for details see refs. [18], [19], and the Experimental Section). The functional capability of the fusion process in our system is demonstrated in Figure 1. In the wide-field fluorescence image a high concentration of fluorescently labelled transducer molecules incorporated into the GUV membrane is visible after a few minutes incubation time with proteoliposomes. For FCS measurements much lower protein concentrations in the GUV were employed. The fusion process was always terminated by replacement of the buffer containing proteoliposomes. The final protein concentration was obtained from the measured autocorrelation curves and was typically between 0.3–3.2 proteins per μm^2. In principle we had no control over the orientation of the incorporated membrane proteins with respect to the GUV membrane and also do not know the orientation of proteins. However, it can be assumed that for Np(SRII–HtrII) binding the relative orientation of both membranes with respect to each other is of importance. Since both possible orientations are represented by subpopulations still with a high number of molecules (in the order of thousand) we can assume that proper complex formation is possible.

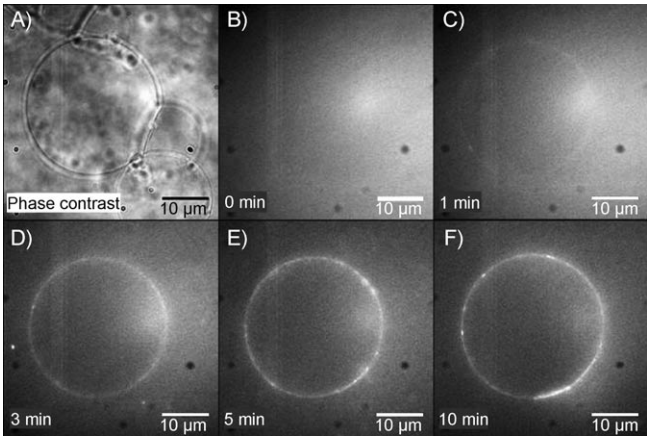

Figure 1. A) A phase contrast and B)–F) a series of wide-field fluorescence images are shown for a GUV loaded with Alexa633-labelled transducer molecules. The fluorescence images were taken at different times after the GUV was incubated with fusion-peptide equipped proteoliposomes (molar protein/lipid ratio 1:2000). At the given concentration of proteoliposomes (which was rather high here) the fusion process was almost completed after 5 min. For subsequent FCS measurements we performed liposome fusion with the GUVs by using a 100-fold diluted proteoliposome solution, which was finally removed by a buffer solution after 10 min in order to decrease background fluorescence of nonfused proteoliposomes.

The lateral protein diffusion in the GUV membrane

Because the measurements were performed at $25 \pm 1\,^{\circ}C$, which is well above the phase transition temperature ($T_c = -2\,^{\circ}C$ for palmitoyl oleoyl phosphatidyl choline [POPC]), the lipids in the GUV are in the liquid phase. Therefore free lateral two-dimensional diffusion can be assumed for the membrane embedded molecules (truncated $NpHtrII_{157}$, NpSRII, and the lipid 1,2-dilinoleoyl-*sn*-glycero-3-phosphoethanolamine [DOPE]), which were first measured separately. The precision of the determined diffusion coefficients relies critically on the accurate vertical positioning of the laser focus with respect to the intersecting upper GUV membrane (Figure 2A). If the laser is not focussed onto the membrane at the correct *z*-position, the divergence of the laser leads to a larger detection area and thereby to a larger radial beam waist *w* and to larger diffusion times. In order to find the correct vertical position of the laser focus a so called *z*-scan has to be performed.[20] For each focal plane along the *z*-axis of the instrument at which the detection volume intersects the GUV surface one measures the fluctuating intensity signals of diffusing molecules from which diffusion times as well as corresponding diffusion coefficients can be obtained. As shown by Hof and co-workers such a *z*-scan can also be used for an intrinsic calibration and absolute diffusion coefficients can be determined without the use of additional reference measurements.[9,20] In a recent study discrepancies in results obtained from the *z*-scan technique and extrinsic calibration are reported; such discrepancies may occur if the confocal detection volume cannot be approximated sufficiently well by a three dimensional Gaussian profile.[21] However, in this study we employed 2fFCS, which makes use of an additional laterally shifted laser focus that is positioned at a known distance with respect to the first focus. Due to the introduction of this external ruler, 2fFCS requires no extrinsic calibration.[17] In 2fFCS the measured data consist of two auto-correlation functions (one for each focus) and one cross-correlation function (across foci) which is fitted globally (for details see the Experimental Section). In most cases the data could be fitted satisfactorily with a one-component two-dimensional diffusion model. For global fits, one fitting parameter describing the radial beam waist *w*, one for the molecule concentration in the detection area, and one for the diffusion coefficient were employed, while the known lateral distance between both foci (403 nm) was fixed.[17] Fitting results obtained from data measured at different *z*-positions are shown in Figure 2B and C. In contrast to *z*-scans with a single beam focus, diffusion times increased with increasing vertical distance (Δz) from the central position of the laser beam with respect to the bilayer plane. In

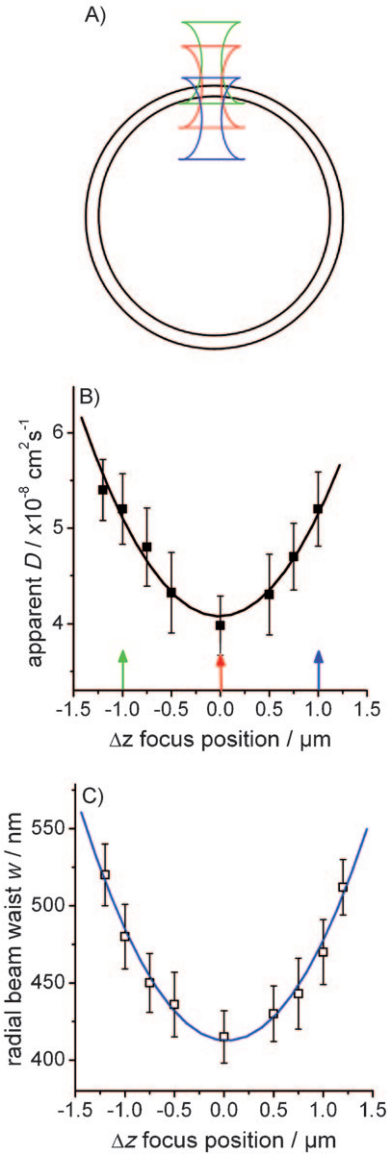

Figure 2. A) Schematic side view of a GUV with intersecting beam foci (red color: central intersection with the GUV surface; green and blue color: non-central intersection with the GUV surface, see also arrows in (B). B), C) Here the typical dependence of the apparent lateral 2D diffusion coefficients and of the radial beam waist on the *z*-position of the laser beam focus is shown for a GUV containing labelled NpHtrII. Each presented data point was a result from a fit of the 2fFCS data (see Experimental Section and Figure 4). The resulting values were fitted with a parabolic curve (solid lines).

2fFCS we observe an increase of apparent diffusion coefficients with increasing Δz. Due to the clipping of the detection volume by the pinhole at larger Δz, we observe effectively that the centres of gravity of the two foci move closer to each other (that is, smaller foci distance δ); this leads to larger apparent diffusion coefficients. However, the minimum values obtained from *z*-scans represent the correct values because they were measured at a position where the projection of the confocal aperture in sample space is significantly wider than the total size of illuminated area.

Table 1. For the three fundamental molecules (DOPE, NpHtrII, NpSRII) the measured lateral two dimensional diffusion coefficients (mean values and the standard deviations of the mean) are shown in this table. For these molecules the cylindrical radii were calculated from the known cross sectional areas of the molecules (for the lipid 70 Å^2, for both membrane proteins based on the crystal structure[4]). In addition, the measured diffusion coefficients are given for two protein mixtures of labelled NpHtrII and nonlabelled NpSRII (for details see section "Intermolecular membrane protein binding" and the Experimental Section). Based on the 1/*R* dependence of the measured diffusion coefficients of these mixtures (see Figure 3), cylindrical radii and cross-sectional areas were obtained by inter- or extrapolation. One can determine which fractions of NpHtrII molecules formed a complex with NpSRII. The values in brackets represent radii and corresponding cross-sectional areas, assuming that NpHtrII has formed a complex with NpSRII to 100%.

	M_W [kDa]	Cylindrical radius [Å]	Cross-sectional area [Å^2]	D_{2D} [cm^{2}s]$^{-1}$
lipid (DOPE)	1.5	4.7	70	$7.9\pm0.35\times10^{-8}$
HtrII	17.4	9.3	271.71	$4.1\pm0.39\times10^{-8}$
SRII	26.5	17.4	951.14	$2.2\pm0.40\times10^{-8}$
1) SRII + HtrII_dye	43.9	12.2 (19.7)	467.59 (1222.85)	$3.1\pm0.46\times10^{-8}$
2) SRII + HtrII_dye	43.9	18.0 (19.7)	1017.87 (1222.85)	$2.1\pm0.48\times10^{-8}$

The diffusion coefficients and the corresponding cylindrical radii from our measurements are given in Table 1 and in Figure 3. The obtained value for lipid diffusion ($D_{2D}=7.9\times10^{-8}$ cm^2 s) is in agreement with recently observed values, also measured with FCS in GUVs.[9,10,21] For NpSRII, comparable data has been published for the very similar Bacteriorhodopsin (BR, also a seven helix membrane spanning integral membrane protein with an almost identical cylindrical radius). The observed diffusion coefficients of BR range from 0.08–1.4$\times10^{-8}$ cm^2 s as measured with FCS or with fluorescence recovery

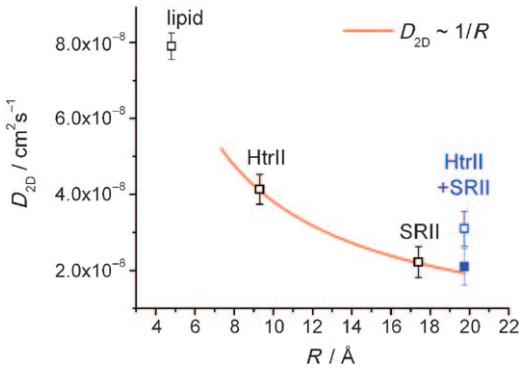

Figure 3. Two-dimensional diffusion coefficients are given as a function of the cylindrical radius of a lipid (DOPE), the transducer, and the receptor (black open squares; values taken from Table 1). The dependence of the lateral diffusion on the cylindrical radius *R* was fitted with a 1/*R* proportionality (red solid line) for the two membrane proteins. The dependence of the diffusion on *R* according to the Saffman-Delbrück model with $D_{saffm}=(k_BT/4\pi\mu_m h)[\ln(\mu_m h/\mu_w R)-0.5772)]$ would show a much weaker *R* dependence (*T*: absolute temperature, μ_w : viscosity of surrounding water, μ_m: viscosity within the lipid matrix, *h*: thickness of the membrane, *R*: cylindrical molecule radius). The blue symbols represent diffusion coefficients of labelled NpHtrII in the presence of unlabelled NpSRII molecules (for more details see section "Intermolecular membrane protein binding").

after photobleaching (FRAP).[19,22,23] Due to the fact that BR is still another protein as compared to NpSRII, that the measurements have been performed partly at rather different protein concentrations, and that FRAP is a technique sensitive to other length and time scales as compared to FCS, we cannot expect a better accordance with the value we obtained for NpSRII ($D_{2D} = 2.2 \times 10^{-8}$ cm^2 s). Within the limits of error, the obtained diffusion coefficients for our membrane proteins do not vary with the protein concentration used in this study. At much higher protein concentrations (molar protein/lipid ratio: 1:2000) as used in a recently published study employing FRET, partial homodimerization was observed for NpHtrII and for NpSRII.[5] However, for the protein concentrations used here (three orders of magnitude lower than those in the FRET study) we do not expect any homodimerization and therefore assume monomeric diffusing molecules.

A theoretical description of particle diffusion in free lipid bilayers was given by Saffman and Delbrück (SD).[24] In this model, cylindrical objects are embedded in a two-dimensional lipid matrix and the observed lateral diffusion is due to thermal motions. According to this model the 2D diffusion coefficient depends only logarithmically on the particle's cylindrical radius R (see legend of Figure 3). Because in SD theory the lipid bilayer is treated as a two-dimensional continuous fluid, reasonable predictions of diffusion coefficients should be expected only from particles significantly larger than the lipid molecules, such as proteins or protein complexes. The obtained two dimensional diffusion coefficients of both membrane proteins are well described by a $1/R$ dependence, and this differs significantly from the classical SD model. This deviation is not unexpected, because the molecule radius of the transducer is only two times larger than a radius of a lipid molecule (see Table 1), and the SD model is valid only for diffusing particles with significant larger radii. A similar $1/R$ behaviour was recently observed by Gambin et al. for various peptides and relatively small transmembrane proteins.[23] This disagreement with the SD model was explained by a breakdown of the hydrodynamic calculation in the case of too small radii of the diffusing particles. However, based on the relativly strong dependence of the diffusion coefficient on the molecule's radius in the regime of $R = 5$–20 Å, we can employ the phenomenological $1/R$ relation to estimate to the degree of the receptor–transducer binding.

Intermolecular membrane protein binding

Based on the above described size-dependent diffusion properties, we investigated the NpSRII/NpHtrII binding by fusing nonlabelled NpSRII molecules together with labelled NpHtrII into the GUVs. For this purpose, transducer molecules and photoreceptor molecules were reconstituted in different proteoliposomes that were subsequently fused into GUVs. Upon Np(HtrII/SRII) binding we would expect a slower diffusion coefficient of NpHtrII as compared to the diffusion of an unbound transducer. Indeed, as shown in Figure 3 (open blue symbol), we clearly observe a significantly slower diffusion in GUVs in which the transducer and the photoreceptor are present together. The corresponding diffusion coefficient of NpHtrII ($3.1 \pm 0.46 \times 10^{-8}$ cm^2 s at 1.4 molecules per μm^2) is already smaller than that one for the single transducer ($4.1 \pm 0.39 \times 10^{-8}$ cm^2 s) and therefore indicates that a fraction of all NpHtrII in the GUV binds NpSRII. In a second set of experiments, we reconstituted labelled transducer and nonlabelled photoreceptors together at the same molar stoichiometry into proteoliposomes and thereafter fused them into GUVs. For this sample we observed an even smaller diffusion coefficient ($2.1 \pm 0.48 \times 10^{-8}$ cm^2 s at 1.2 molecules per μm^2), which is rather close to a value predicted from the $1/R$ dependence of the Np(HtrII/SRII) structure (solid blue symbol in Figure 3). The latter result indicates that at the given protein concentration (molar protein/lipid ratio ~1: 2000000) nearly 80% of the transducer molecules form a Np(SRII/HtrII) complex with the related photoreceptor (see the Experimental Section). Most probably, in the first experiment we do observe only a partial NpHtrII/NpSRII complex formation (~20% complexes), because NpSRII-loaded proteoliposomes did not fuse to GUVs to the same extent as NpHtrII-loaded liposomes. In the second approach the equal stoichiometry of NpHtrII and NpSRII is guaranteed intrinsically.

Conclusion

In the present study we demonstrated that measuring lateral diffusion of integral membrane proteins with a sufficient precision is a fruitful method to quantify the degree of intermolecular binding or oligomerization of membrane proteins at almost physiological protein concentration in lipid bilayer systems. We showed that intermolecular binding between the photoreceptor NpSRII and its related transducer NpHtrII is extremely strong because we observe heterodimeric complexes in giant vesicles with a 20 μm diameter in which only ~1000 membrane proteins of each type are present. Future studies with full length transducers should offer the possibility to study the NpHtrII-NpHtrII binding; this would provide insight into the topology of the functional photo-signalling complex. By using this technique in the future, we can analyze receptor–signalling complexes as part of the signalling cascade; these are supposed to form higher order structures or clusters.[25–27] It appears that 2fFCS applied to diffusing proteins in GUVs is a valuable technique to obtain information about unperturbed membrane proteins.

Experimental Section

Protein expression, cysteine mutants and labeling with fluorophores: Expression of the photoreceptor NpSRII and the N-terminal fragment of the transducer NpHtrII consisting of residues 1–157 ($NpHtr_{157}$), was carried out in *E. coli*. For purification purposes, both proteins carry a C-terminal His_7-tag. Cysteine mutations were introduced by using the overlap extension method and details on protein expression and purification were described in earlier work.[3,28] Cysteine mutants were labelled with maleimide-functionalized dyes (Alexa633 from Invitrogen, Karlsruhe, Germany). Purified protein (2–10 μM) was dialysed against our standard buffer (10 mM Tris-HCl, 150 mM NaCl, 0.05% DDM, pH 7.4) for 24 h. In this buffer the proteins react with a three- to sevenfold excess of dye overnight a 4 °C. Unbound dye was removed using a gel-filtration

column (Sephadex G-25, Amersham Biosciences). Further details on determination of label ratios are described elsewhere.[5]

GUV preparation and protein transfer into GUV: GUV preparation was performed by using the electroformation technique described by Angelova and Dimitrov.[29] A solution of POPC (1 mg mL^{-1}) in chloroform with 1,2-dilinoleoyl-*sn*-glycero-3-ethlphosphocholine (EDOPC, 0.5 mol%) and biotinyl-DOPE (0.1 mol%) was deposited on an indium tin oxide (ITO)-coated cover glass, and the solvent was evaporated under vacuum for 30 min. A neutravidin (Pierce Biotechnology Inc., Rockford, IL, USA) solution (0.1 mg mL^{-1}, 500 μL) was placed on a second ITO-coated glass slide, and was dried for 15 min under nitrogen flow. Subsequently, both ITO-coated slides, a silicon gasket, and two stripes of a self-adhesive copper foil were employed to form a closed chamber. Through an inlet port a glucose solution (300 μL, 111 mM) was filled into the chamber. An alternating current (1.5 V at 15 Hz) was applied to the chamber for two hours. After this time GUVs were formed and the chamber was flushed carefully and incubated for 1 h with a saccharose solution (111 mM). Because of the lower specific density of the encapsulated glucose solution inside the GUV they ascend and biotinylated lipids in the GUVs bound to the neutravidin layer of the upper cover slide. After immobilizing individual GUVs (with 20–40 μm in diameter) on the upper cover slide, the chamber was turned headlong and the glucose buffer was exchanged with standard buffer (50 mM NaCl, 10 mM Tris, pH 7.4). In order to incorporate membrane proteins into GUVs, proteoliposomes were fused with GUV.[18,19] For this purpose liposomes were made from DOPE-PDP and POPC (1:20 mol/mol) with a radius of about 100 nm, and membrane proteins were reconstituted into the vesicles at a molar protein-to-lipid ratio of 1:2000 (for details see ref. [5]). The fusion peptide WAE-11 (synthesized by JPT Technologies, Berlin, Germany) was bound to the proteoliposomes through a disulfide bridge before the liposomes were fused into GUV.[18] A successful incorporation of fluorescently labelled membrane proteins was monitored by a time series of fluorescence wide-field exposures (see Figure 1).

GUV imaging and FCS measurements: Surface-tethered GUVs with incorporated fluorescently labelled membrane proteins were imaged by employing an inverted microscope (Olympus IX-71) in wide-field illumination mode. Excitation light at 640 nm was provided by an argon-ion laser-pumped dye laser (Radiant Dye Laser & Accessories GmbH, Wermelskirchen, Germany). The light was reflected by a dichroic mirror (Q660LP, Chroma Technology, Rockingham, VT, USA) into the high numerical aperture objective. Fluorescence emission was collected by an UPlan 1.3 N.A./×100 oil-immersion objective (Olympus, Hamburg, Germany), passed through a discriminating filter (690DF40, Omega Optical, Brattenboro, USA), and imaged onto a high-sensitivity Peltier-cooled CCD camera (iXon DV885, Andor Technology, South Windsor, CT, USA).

Diffusion coefficients were measured at room temperature (25 ± 1 °C) by using the recently developed 2fFCS.[17] Two alternately pulsing laser diodes (LDH-P-635, PicoQuant, Berlin, Germany) emit light beams at 640 nm that are linear polarized, but orthogonal to each other. The light of both diodes is combined into a single beam by employing a polarizing beam splitter (narrow band polarizing beam splitter cube 633, Ealing, St. Aspah, UK). The light is reflected by a dichroic mirror (Q660LP, Chroma Technology, Rockingham, VT, USA) and subsequently passed through a DIC-prism (U-DICTHC, Olympus, Hamburg, Germany) into a high numerical aperture objective (UPLAPO 1.3 N:A/60x water immersion). Due to different polarization orientations for each laser pulse, we obtain two laterally shifted and overlapping laser foci at a fixed and known distance (400 nm). Collected emission light from each focus is imaged into a pinhole (200 μm), collimated, split by a 50/50 beam splitter, and finally detected by two single photo avalanche diodes (SPCM-AQR-14, Perkin–Elmer, Wellesley, MA, USA). In addition to the setup described above, we also performed 2fFCS measurements with an adapted MicroTime 200 from PicoQuant (Berlin, Germany; for details see Application Note "AppNote 2fFCS", PicoQuant 2007). The power of the exciting laser was ~1 μW in order to avoid photobleaching of the fluorophores. The measuring time was generally between ten and 20 min for each *z*-position as part of a whole *z*-scan. In some cases, high intensity bursts, which most probably represent larger protein aggregates but show up rarely, were cleaned from time traces. The measured data was processed, analyzed, and displayed with the software SymPhoTime (PicoQuant, Berlin, Germany), with custom written *Matlab* routines, and with OriginPro 7.5 (OriginLab Corp., Northhampton, MA, USA).

Calibration and determination of diffusion coefficients: Calibration measurements of the setup were performed with Alexa633 freely diffusing in solution. Subsequently lateral diffusion of fluorescently labelled molecules was measured for different *z*-positions above the cover slide surface. Using a model for two-dimensional diffusion, we fitted simultaneously two autocorrelation (ACF for each focus) and a cross-correlation (CCF between both foci) function(s) to the measured data and determined related diffusion coefficients (see Figure 4 and ref. [17] for more details). For purely two-dimensional diffusion, the data were fitted by using Equations (1) and (2)]:

$$G_{CCF}(t,\delta) = G_\infty(\delta) + \frac{\pi\varepsilon^2 c}{4}\frac{1}{4Dt+w^2}\exp\left(-\frac{\delta^2}{4Dt+w^2}\right) \quad (1)$$

and

$$G_{ACF}(t) = G_\infty + \frac{\pi\varepsilon^2 c}{4}\frac{1}{4Dt+w^2} \quad (2)$$

in which G_∞ is an offset value, D is the two dimensional diffusion coefficient, w is the radial diameter of the Gaussian detection vol-

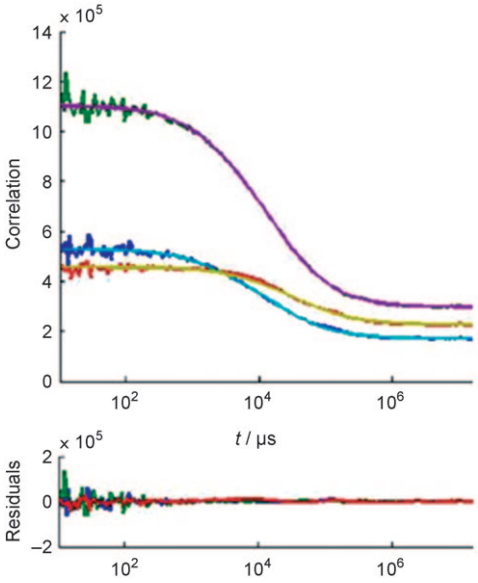

Figure 4. The two autocorrelation functions (blue and green lines) and a cross-correlation function (red line) were calculated from data recorded for laterally diffusing NpHtrII using 2fFCS setup. The correlation functions were fitted with a model for two-dimensional diffusion and the result of the global fit is shown with the corresponding fitting curves.

umes, δ the distance between both foci, c the molecule concentration per area, and ε a parameter describing the overall excitation power times detection efficiency. With the known value of $\delta =$ 403 nm, c, ε, w, and D were the fit parameters. In the case of planar membranes intersecting the focus beam at different z-positions the dependence of the beam waist on z is given by Equation (3):

$$w(z) = w_0\left[1 + \left(\frac{\lambda_{ex} z}{\pi w_0^2 n}\right)^2\right]^{1/2} \quad (3)$$

Here w_0 is the beam waist in the focal plane, λ_{ex} is the excitation wavelength, and n is the refractive index of the immersion medium (water). Resulting beam waists and corresponding diffusion coefficients as obtained from data measured at different z-positions are shown in Figure 2B and C. All presented diffusion coefficients and corresponding standard deviations (Table 1, Figure 3A) were obtained from four to eight individual z-scans as measured in different GUVs. According to Hof and co-workers,[9] for some z-scans the diffusion coefficients were calculated from autocorrelation functions by taking the minimum values of the parabolic dependence on the z-position by using Equation (4):

$$\tau_D = \frac{\omega_0^2}{4D}\left[1 + \left(\frac{\lambda_{ex} z}{\pi w_0^2 n}\right)^2\right] \quad (4)$$

The diffusion coefficients obtained from z-scans by using a single focus were the same compared to those obtained from 2fFCS within the limits of error (see also ref. [30]).

Calculation of the complex-forming transducer fraction: In principle the fraction of complex-forming NpHtrII can be determined by the use of a two-component fit—one component for only NpHtrII and one for the Np(HtrII/SRII) complex. Unfortunately the difference in diffusion coefficients between pure NpHtrII and Np(HtrII/SRII) complexes was too small for a successful application of this approach. Therefore we also fitted the data from measurements with both proteins in the GUV with a single component and extracted a single diffusion coefficient, which represents a mean value originating from two subpopulations. Based on the known molecular structure, a cross-sectional area and the corresponding cylindrical radius were calculated for both diffusing membrane proteins (A_{Htr}, A_{SR}) as given in Table 1. The fraction of transducer molecules that form Np(Htr/SRII) complexes was estimated by using interpolated or extrapolated radius values (respectively the cross sectional area values A_{meas}) as obtained from the $1/R$ dependence (see Figure 3). The expected cross-sectional area for the complex (NpHtrII plus NpSRII) is 1222.85 Å^2, which corresponds to a cylindrical radius of 19.7 Å if all transducers in the sample form a complex. Because we observed experimentally smaller values for samples with NpHtrII and NpSRII in the GUVs for both measurements with Np(HtrII/SRII) mixtures, complex formation is not 100%. The resulting fraction of transducers that form complexes (f_{comp}) is calculated as follows [Eq. (5)]:

$$f_{comp} = \frac{A_{meas} - A_{Htr}}{A_{SR}} \quad (5)$$

Using this relation we obtained $f_{comp} = 0.21$ for the first measurement and $f_{comp} = 0.78$ for the second measurement with Np(HtrII/SRII) mixtures in the GUV.

Abbreviations: EDOPC: 1,2-dilinoleoyl-*sn*-glycero-3-ethlphosphocholine; EPR: electron paramagnetic resonance; FCS: fluorescence correlation spectroscopy; FRAP: fluorescence recovery after photobleaching; FRET: Förster resonance energy transfer; GUV: giant unilameller vesicle; DOPE: 1,2-dilinoleoyl-*sn*-glycero-3-phosphoethanolamine; NpHtrII: *Natronomonas pharaonis* transducer of sensory rhodopsin II; NpSrII: *Natronomonas pharaonis* sensory rhodopsin II; ITO: indium tin oxide; POPC: palmitoyl oleoyl phosphatidyl choline.

Acknowledgements

The priority program SPP 1128 of Deutsche Forschungsgemeinschaft (FI 841/3-1,2 to J.F. and to J.E.) and the DFG graduate school 1035 "Biointerface" are acknowledged for funding. We thank B. Kaupp and G. Büldt for continuous support in their institutes.

Keywords: fluorescence spectroscopy · giant unilamellar vesicles · membrane proteins · photo-signaling complexes · protein diffusion

[1] J. L. Spudich, H. Luecke, *Curr. Opin. Struct. Biol.* **2002**, *12*, 540–546.
[2] J. P. Klare, V. I. Gordeliy, J. Labahn, G. Buldt, H. J. Steinhoff, M. Engelhard, *FEBS Lett.* **2004**, *564*, 219–224.
[3] A. A. Wegener, J. P. Klare, M. Engelhard, H. J. Steinhoff, *EMBO J.* **2001**, *20*, 5312–5319.
[4] V. I. Gordeliy, J. Labahn, R. Moukhametzianov, R. Efremov, J. Granzin, R. Schlesinger, G. Buldt, T. Savopol, A. J. Scheidig, J. P. Klare, M. Engelhard, *Nature* **2002**, *419*, 484–487.
[5] J. Kriegsmann, M. Brehs, J. P. Klare, M. Engelhard, J. Fitter, *Biochim. Biophys. Acta, Biomembr.* **2009**, *1788*, 522–531.
[6] J. Otomo, W. Marwan, D. Oesterhelt, H. Desel, R. Uhl, *J. Bacteriol.* **1989**, *171*, 2155–2159.
[7] T. Baumgart, S. T. Hess, W. W. Webb, *Nature* **2003**, *425*, 821–824.
[8] D. Merkle, N. Kahya, P. Schwille, *ChemBioChem* **2008**, *9*, 2673–2681.
[9] M. Przybylo, J. Sykora, J. Humpolickova, A. Benda, A. Zan, M. Hof, *Langmuir* **2006**, *22*, 9096–9099.
[10] L. Guo, J. Y. Har, J. Sankaran, Y. Hong, B. Kannan, T. Wohland, *ChemPhysChem* **2008**, *9*, 721–728.
[11] N. Kahya, D. A. Wiersma, B. Poolman, D. Hoekstra, *J. Biol. Chem.* **2002**, *277*, 39304–39311.
[12] M. K. Doeven, J. H. Folgering, V. Krasnikov, E. R. Geertsma, G. van den Bogaart, B. Poolman, *Biophys. J.* **2005**, *88*, 1134–1142.
[13] M. K. Doeven, G. van den Bogaart, V. Krasnikov, B. Poolman, *Biophys. J.* **2008**, *94*, 3956–3965.
[14] E. Thews, M. Gerken, R. Eckert, J. Zapfel, C. Tietz, J. Wrachtrup, *Biophys. J.* **2005**, *89*, 2069–2076.
[15] A. J. Garcia-Saez, P. Schwille, *Appl. Microbiol. Biotechnol.* **2007**, *76*, 257–266.
[16] J. Ries, P. Schwille, *Phys. Chem. Chem. Phys.* **2008**, *10*, 3487–3497.
[17] T. Dertinger, V. Pacheco, I. der Hocht, R. Hartmann, I. Gregor, J. Enderlein, *ChemPhysChem* **2007**, *8*, 433–443.
[18] E. I. Pecheur, D. Hoekstra, J. Sainte-Marie, L. Maurin, A. Bienvenue, J. R. Philippot, *Biochemistry* **1997**, *36*, 3773–3781.
[19] N. Kahya, E. I. Pecheur, W. P. de Boeij, D. A. Wiersma, D. Hoekstra, *Biophys. J.* **2001**, *81*, 1464–1474.
[20] A. Benda, M. Benes, V. Marecek, A. Lhotsky, W. T. Hermens, M. Hof, *Langmuir* **2003**, *19*, 4120–4126.
[21] E. Gielen, M. Vandeven, A. Margineanu, P. Dedecker, M. Van der Auweraer, Y. Engelborghs, J. Hofkens, M. Ameloot, *Chem. Phys. Lett.* **2009**, *469*, 110–114.
[22] R. Peters, R. J. Cherry, *Proc. Natl. Acad. Sci. USA* **1982**, *79*, 4317–4321.
[23] Y. Gambin, R. Lope *z*-Esparza, M. Reffay, E. Sierecki, N. S. Gov, M. Genest, R. S. Hodges, W. Urbach, *Proc. Natl. Acad. Sci. USA* **2006**, 103, 2098–2102.
[24] P. G. Saffman, M. Delbrück, *Proc. Natl. Acad. Sci. USA* **1975**, *72*, 3111–3113.
[25] J. J. Falke, G. L. Hazelbauer, *Trends Biochem. Sci.* **2001**, *26*, 257–265.

[26] T. S. Shimizu, N. Le Novere, M. D. Levin, A. J. Beavil, B. J. Sutton, D. Bray, *Nat. Cell Biol.* **2000**, *2*, 792–796.
[27] V. Sourjik, H. C. Berg, *Nature* **2004**, *428*, 437–441.
[28] I. P. Hohenfeld, A. A. Wegener, M. Engelhard, *FEBS Lett.* **1999**, *442*, 198–202.
[29] M. I. Angelova, D. S. Dimitrov, *Faraday Discuss. Chem. Soc.* **1986**, *81*, 303–308.
[30] T. Dertinger, I. von der Hocht, A. Benda, M. Hof, J. Enderlein, *Langmuir* **2006**, *22*, 9339–9344.

Received: April 23, 2009
Published online on June 23, 2009

